

Optical Trapping

S. Rager (sr3874)¹

¹PHYSUN3801 Columbia University

(Dated: 23:13 Tuesday 10th December, 2024)

To observe Brownian motion under a microscope and trap various sizes of poly beads using laser light in order to calculate the trapping force of the laser.

AIM

To observe Brownian motion under a microscope and trap various sizes of poly beads using laser light.

INTRODUCTION & METHOD

Dr. Ashkin reported "the first experimental observation... of a single-beam gradient force radiation pressure particle trap" in a 1986 paper after observing particles "stick" to a laser beam he had focused on a sample of particles while he was observing them through a microscope. This is in contrast to the otherwise Brownian motion of the particles. This result led to objects smaller than ten microns being able to be manipulated with a beam of light. Furthermore, since the shape of the potential energy well is well characterized, forces on the order of piconewtons are measurable with this approach, dubbed "Laser Tweezing".

In this instance, the laser tweezer setup used a Melles Griot 05-LHP-925 laser with maximum output of 632.8 nm photons at 30mW. Then, two mirrors, M_1 and M_2 in the diagram of FIG. 1, were used to couple the beam into a telescoping lens set, L_1 and L_2 in the diagram, used to broaden the diameter of the beam.

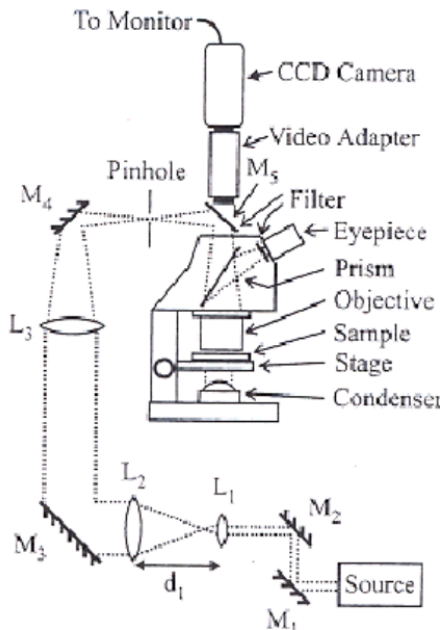


FIG. 1. Laser Tweezer Setup

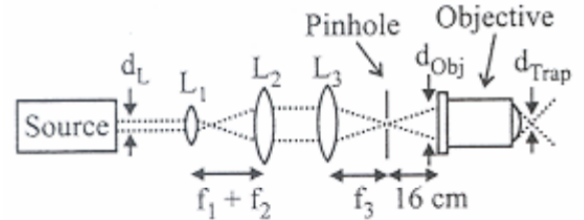


FIG. 2. Laser Tweezer Lens Setup

The telescope is designed to create a beam diameter equal to the diameter of the back of the microscope objective such that there is no power loss on entering the objective and the laser light entirely fills the back of the objective allowing the smallest spot possible to be resolved. A third mirror, M_3 vertically redirects the beam through a third lens, L_3 , giving the beam front the optimal radius of curvature. This optimal radius of curvature is chosen such that it maximizes the focusing power of the objective. Next, the beam strikes a fourth mirror, M_4 , and is directed through a pinhole of an aluminum adapter set on top of the microscope to hold two dichroic reflectors and the charge-coupled device camera used for viewing the output of the microscope on a computer. The dichroic reflectors act as mirrors for long wavelength light while being transparent for light of lower wavelength. Therefore, the laser beam is reflected down onto the sample, but the sample can be backlit and viewed with a camera from above. When the laser is reflected back towards the camera, the dichroic mirrors act to weaken the intensity of the beam in order to prevent damaging the camera. Finally, the objective creates a highly focused spot which acts as an optical trap. FIG. 2 shows just the lens set up of the system and the resulting highly focused spot at d_{Trap} . Note the set up used in the experiment did not have an eyepiece as in FIG. 1.

Once all of the optics were aligned as above such that the objective rendered a highly focused spot on a sample microscope slide, in this case a fly wing, a solution of poly beads was made. The provided poly bead sizes were 1, 2, 3, 6, and 10 microns. To make a solution, approximately 10 ml of distilled water were added to a graduated cylinder. If it was deemed that a more dilute solution was required for better measurements, 5-20 ml of distilled water was added to the graduated cylinder. A bead size was chosen and its respective dropper bottle was taken out of the refrigerator, shaken until the beads entered suspension, and

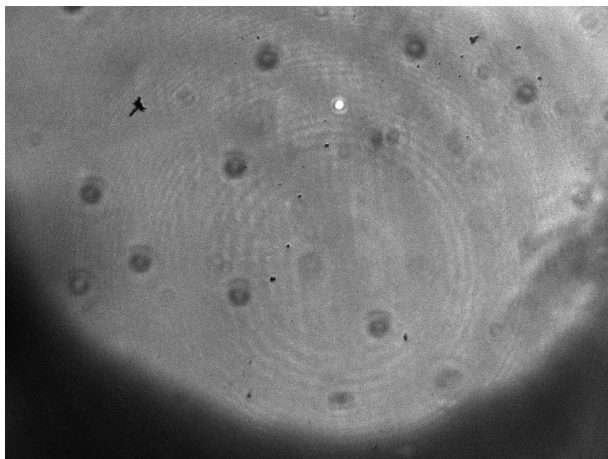


FIG. 3. First Image from New CCD Camera

then added to the graduated cylinder. A single drop was added to begin with. If a more concentrated solution was desired, more drops were then added. A glass transfer pipette with a rubber bulb was used to mix the contents of the graduated cylinder until they formed a homogeneous suspension. Next, high vacuum grease was placed on the edges of a cover slip and the transfer pipette was used to transfer the suspension to the cover slip such that it covered the inside of the well formed by the vacuum grease. A microscope slide was then placed on top of the cover slip.

The actual measurements consisted first of observing the particles were moving in a Brownian fashion in the suspension by focusing the microscope, then of turning on the laser and translating the metal plate holding the slide under the microscope to trap a particle. Once a particle was trapped while the other particles remained Brownian, the plate was again translated to give the trapped particle a "relative" velocity such that the Stoke's drag equation could be used to find the trapping force of the optical trap. This procedure was recorded by the CCD camera and repeated for the various sizes of poly beads.

Finally, a new CCD camera, Allied-Vision's Alvium G1, was installed once all of the data had been collected with the original CCD camera in the hope that higher quality data could be collected with the new camera. It is thought that a black and white output will offer higher contrast and better particle detection. The procedure for switching out the cameras was to solder the power connections to the new camera, remove the old camera and the lens attached to it, attach the lens to the new camera, and place the new camera and lens back on top of the aluminum adapter. Once this was done, the power and RJ45 cables were connect and the Vimba software downloaded. The first image taken with the new camera can be found in FIG. 3. It is noted, however, that the new camera becomes very warm to the touch while in operation.

RESULTS & ANALYSIS

Brownian Motion

FIGs. 4-7 plot the square displacement for particles of 1, 2, and 3 micron radii. The mean square displacement is given by the blue line at the top of the legend with (Mean) in parenthesis in each plot. The words (Red-Tinted) in the legend indicated which particles have been trapped by the laser beam. It is expected with Brownian motion that the mean square displacement of particles increases with the length of the time interval and this can be seen in the plots. The clearest increase is that of FIG. 6 corresponding to the 2 micron poly beads. It is also noted that the mean square displacement almost reaches a "saturation" level because, in the video the plot is derived from, more particles get trapped by the laser as time goes on. This can also be seen in the legend where there are labels such as Particle 5 and Particle 5 (Red-Tinted) indicating that identified particle 5 becomes trapped by the laser. The large spike and dip in the mean square displacement is because the program written to analyze the videos occasionally loses track of a particle or misidentifies it. Note a range of uncertainties and an average uncertainty are provided in the captions because the uncertainties are relatively small and the figures are already quite involved without being obscured by error bars. FIG. 4 is essentially a null result for confirming Brownian motion because the mean square displacement is essentially constant in time. FIG. 4 also shows that the program lost track of multiple particles because the plots for their squared displacement simply end. In order to correct this, the minimum particle radius detected by the program was decreased to produce FIG. 5. FIG. 5 shows that the mean squared displacement increases with time, but there are many more particles being tracked than in FIG. 4 and the plot becomes harder to read. So much so, that the legend has been cropped. Similarly, the legend was cropped in FIG. 7, but it is clear to see that the mean squared displacement increases with time. The Google Colab used for this analysis is provided at the Google Drive link found as the first reference in the references section. The Google Drive link also contains all of the data used and results generated. The Brownian section of the Colab outputs plots using Matplotlib as can be found here. It also outputs the input videos with annotations to display particle velocities and mean square displacements in "real" time as well as csv files containing all of the data. Full data on the uncertainties associated with these calculations may also be found in the csv files generated by this cell of code. Finally, interactive plots similar to the plots here but with zoom, on hover, and trace selection functionality are outputted. The zoom, on hover, and trace selection functionality make it much easier to see that the mean squared displacement increases with time and when particles become trapped their squared displacement goes to zero. This last point is

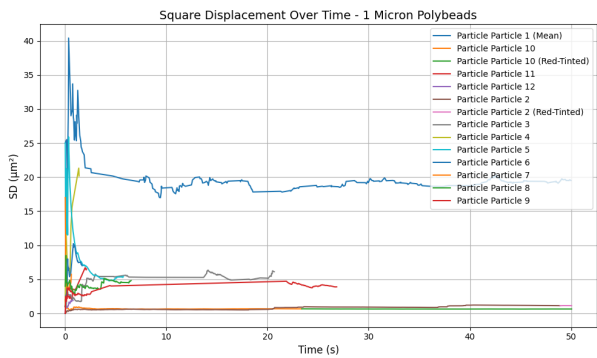


FIG. 4. 1 Micron Mean Square Displacement (Uncertainty Range: [0,3] Microns, Average Uncertainty: 1.45 Microns)

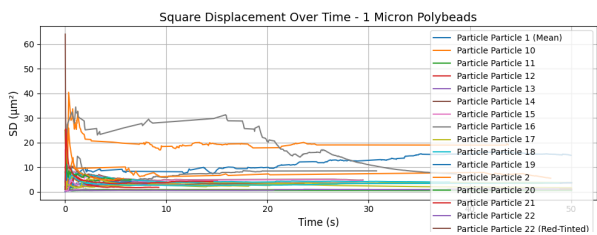


FIG. 5. 1 Micron Mean Square Displacement (Uncertainty Range: [0,3] Microns, Average Uncertainty: 1.63 Microns)

difficult to see in the plots shown here because there are many particles with small displacements obscuring this trend. The Colab also contains an explanation of how the code works and how to run it for one's self. Finally, it is noted that Brownian motion was most clearly observed for particles of smaller radii and was much more faint, almost vibrational, for larger particles.

Radial Trapping Force

The radial trapping force was found by trapping a particle then translating the staging area of the microscope by hand until the particle escaped the trap. Since the particle escapes that trap when the force of drag from the water in the suspension is equal to the

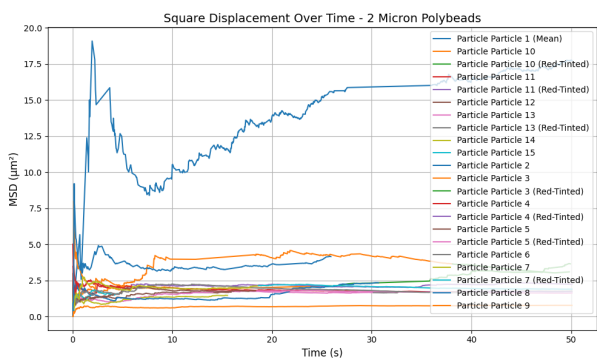


FIG. 6. 2 Micron Mean Square Displacement (Uncertainty Range: [0,3] Microns, Average Uncertainty: 1.75 Microns)

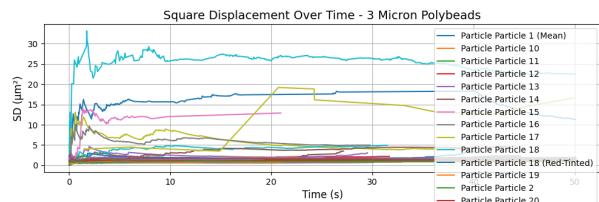


FIG. 7. 3 Micron Mean Square Displacement (Uncertainty Range: [0,3] Microns, Average Uncertainty: 1.73 Microns)

force of the trap, the force of the trap may be found using Stoke's drag equation

$$F = 6\pi r\eta v$$

where F is the force, r is the radius of the particle, η is the fluid viscosity, and v is the escape velocity. $\eta = 10^{-3}\text{Ns}/\text{m}^2$ for water. The code from the Brownian drop down of the Colab was modified for the purposes of this analysis to simply output annotated videos and csv files. The output video for R_2m may be found in the Google Drive, but R_6m does not have an output video because R_6m is a .avi file. Then, basic manipulations were performed on these files to output the average velocity and velocity uncertainty for each particle size, from which the force and force uncertainty were calculated. All of this may be found in the Radial drop down of the Colab. It is noted that videos for particles of all sizes were input into the program, but the quality of data was not particularly good for any sizes besides 2 and 6 microns. The focus of the laser for the 1 micron video was too faint to be detected and the displacements too slight to be detected by the program. The 10 micron video also had the issue of the 10 micron particles becoming stuck to the walls of the slide. It was found that adding 1 micron particles to the suspension of 10 micron particles broke the 10 micron particles off the walls of the slide, allowing the 10 micron particles to be tweezed by increasing the number of collisions experienced by the 10 micron particles. An interesting extension of this experiment would be to use knowledge of the trapping force and the average force due to collisions experienced by the 10 micron particles to calculate the Van der Waals forces between the 10 micron particles and the walls of the slide.

Furthermore, the expected optical tweezing force is able to be calculated from theory. Generally, there are two components to this force. One component involves the gradient of the intensity of the beam and the other is the scattering force. Since the scattering force is on the order of 10^{-17} its contribution has been ignored in these calculations. The z-component has also been ignored since good data was taken only in the radial plane. Therefore,

$$F_{\text{grad}} = \frac{-2\pi n_m^2 a^3}{c} \frac{n_p^2 - n_m^2}{n_p^2 + 2n_m^2} \frac{8P}{\pi \omega^4} r e^{-\frac{2r^2}{\omega^2}}$$

where $n_p = 1.59$ is the refractive index of polystyrene, $n_m = 1.33$ is the refractive index of water, a is the

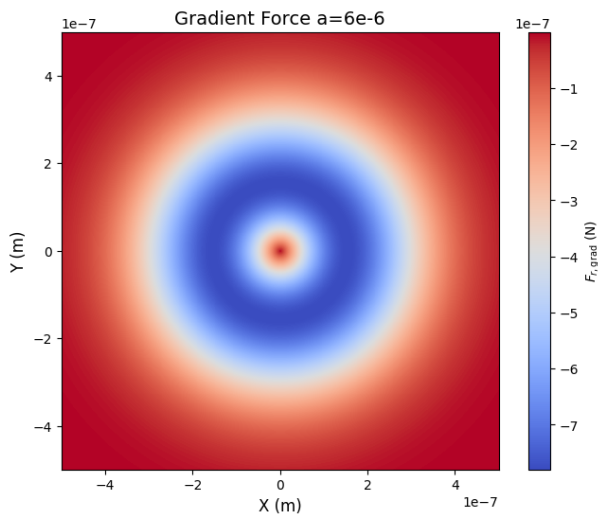


FIG. 8.

radius of the particle, c is the speed of light, P is the power of the laser, and ω is the minimum beam waist. See reference V. for more details. The beam waist is given by $\omega = \frac{2\lambda f}{\pi d}$ with λ being the wavelength of light, f the focal length of the objective, and d the diameter of the beam. In this case d equals the diameter of the objective lens. The focal length $f=4\text{mm}$ was written on the barrel of the Bausch Rochester JP3595 objective, but information on the lens diameter was not obtainable. Therefore, the lens diameter and also the beam diameter are estimated by the entrance pupil diameter and $d=2 \text{ N.A. } f$ where N.A. is the numerical aperture and f is the focal length. The approximation that the effective focal length equals the focal length has been made in the previous equation. The numerical aperture found on the barrel of the objective was 0.65. FIG 8. shows a plot of F_{grad} for $a=6$ microns in the radial plane. Notice the force drops off to zero after a certain radius and there is a restorative force directed towards the origin where a particle once again experiences no force. A value of $r = \frac{a}{\frac{\log a}{\log(2)} e}$ was used to derive F_{grad} as found in the following table in order to get a sense of the expected order of magnitude. This value was chosen because F_{grad} decays exponentially. The logarithm prefactor in the denominator is chosen to approximately correct for the fact that particles escape the optical trap at different radii depending on the radii of the particles. This worked well for the 2 micron particles and gave forces that agree to within 7% but poorly for the 6 micron particles with the predicted F_{grad} being less than half of the calculated force. Note, however, that the goal of calculating F_{grad} from theory was to establish an expected magnitude for the results and all

force magnitudes are on the order of piconewtons.

| Video | Velocity ($\mu\text{m/s}$) | Velocity Uncertainty ($\mu\text{m/s}$) | Force (pN) | Force Uncertainty (pN) | F_{grad} (pN) |
|-------|------------------------------|--|------------|------------------------|-----------------|
| R_2m | 66.91 | 2.77 | 2.52 | 0.11 | 2.69 |
| R_6m | 28.98 | 2.83 | 3.28 | 0.32 | 1.55 |

CONCLUSIONS

Brownian motion of poly beads of 1, 2, and 3 radii was observed. An optical trap was constructed and poly beads of radii 1, 2, 3, 6, and 10 microns were trapped. The trapping force of this set up was measured for poly beads of radii 2 and 6 microns. In the radial direction this force was measured to be 2.9 pN, averaged between the 2 and 6 micron cases. The average of the two cases for the estimated gradient force from theory was 2.12 pN which is slightly less than three fourths the measured average.

ACKNOWLEDGEMENTS

Benjamin Graeme Gorman (bgg2112), Quinn Manning (jqm2108), and Alvin Wang (ahw2147) for their contributions as my lab partners

I. Optical Trapping Data & Analysis, accessed Tuesday 10th December, 2024, <<https://drive.google.com/drive/folders/1r6tCrijdmC0SwljzmJbzgc6kOWLm8AE>>.

II. PHYSUN3081 Spring 2020 Intermediate Laboratory Work Laser Tweezer, accessed Tuesday 10th December, 2024, <https://www.columbia.edu/~mm21/exp_files/Laser%20Tweezers.pdf>.

III. EKA Advanced Physics Laboratory Course, accessed Tuesday 10th December, 2024, <<http://tesla.phys.columbia.edu:8080/eka/>>.

IV. Melles Griot 05-LHP Datasheet ArtisanTG, accessed Tuesday 10th December, 2024, <https://www.artisanTG.com/info/Melles.Griot_05_LHP_Datasheet_2019731111233.pdf?srsltid=AfmBOoqpdJcp6yOv9Oj1bC4NmjpGfIhrOAwH5znAB6DzxjNbBnSxfZ1q>.

V. Yasuhiro Harada, Toshimitsu Asakura, Radiation forces on a dielectric sphere in the Rayleigh scattering regime, Optics Communications, Volume 124, Issues 5–6, 1996, Pages 529-541, ISSN 0030-4018, [https://doi.org/10.1016/0030-4018\(95\)00753-9](https://doi.org/10.1016/0030-4018(95)00753-9). <<https://www.sciencedirect.com/science/article/pii/0030401895007539>>